THE JOURNAL OF PHYSICAL CHEMISTRY C

pubs.acs.org/JPCC

Article

Photoluminescence and Stoichiometry Correlation in Nanocrystalline EuO_x Thin Films: Tunable Color Emission

Antonio Mariscal-Jiménez,* Aitana Tarazaga Martín-Luengo, Beatriz Galiana, Carmen Ballesteros, Alberta Bonanni, Javier Martín-Sánchez,* and Rosalía Serna*

Cite This: *J. Phys. Chem. C* 2020, 124, 15434−15439

Read Online

ACCESS | Metrics & More | Article Recommendations | Supporting Information

ABSTRACT: The development of broadband and ultracompact optoelectronic devices relies on the possibility of fabricating bright and tunable emitters at the nanoscale. Here, we show emission from EuO_x ($1 \leq x < 1.4$) thin films on silicon formed by nanocrystals with average sizes in the range of 5 nm. The photoluminescence emission of the nano-EuO_x films is tunable as a function of the oxygen concentration changing from a green broadband Eu^{2+}-related emission to a narrow red Eu^{3+}-related emission. To reach these results has been instrumental through the use of a new methodology specially designed to achieve high-quality europium oxide films whose compositional properties are controlled by the growth base pressure and preserved thanks to a chemically stable and transparent cover layer of Al_2O_3. Our findings confirm the outstanding potential of nanostructured EuO_x films as "one-compound" optical elements with tunable emission properties for their implementation in integrated silicon-based devices.

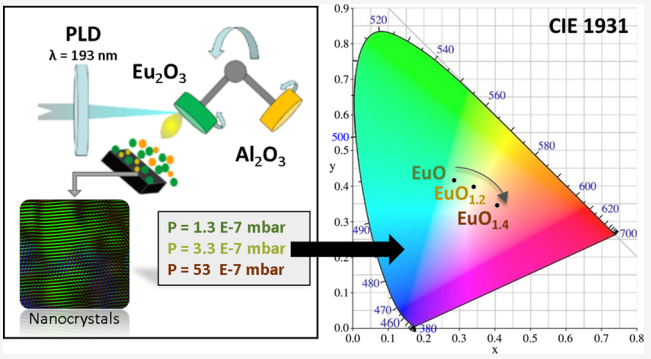

INTRODUCTION

Luminescence from rare earth Eu (europium) ions holds great promises for applications compatible with silicon technologies, such as optical recording and encryption,[1] white cathodoluminescence emission,[2] and phosphors with excellent stability and color performance.[3] To answer this interest, Eu-doping in Si-based materials has been a very active field of research that has included studies not only of the photoinduced luminescence[4] but also of the electrical excitation of oxides suitable for Si integration doped with trivalent Eu (Eu^{3+}),[5] and more recently, the cathodoluminescence of oxides and oxynitrides doped with divalent Eu (Eu^{2+}) has been reported.[6] In this context, the photoluminescence of europium oxides has been less investigated, although they hold a great potential for different optoelectronic applications. While the europium trioxide (Eu_2O_3) is a wide band gap oxide relevant mainly for lighting applications, such as sensitization in lanthanide-doped inorganic nanocrystals,[7] additive-free red-emitting transparent ceramics,[8] high quantum efficiency phosphors,[9] dense translucent ceramics,[10] and much more, the europium monoxide (EuO) is a ferromagnetic semiconductor[11] showing interesting magnetic properties, becoming ferromagnetic below a Curie temperature at 69 K.[12] Recently, for example, inducing magnetism by proximity in two-dimensional materials such as graphene has been reported.[13] Moreover, europium monoxide belongs to a compact group of magnetic semiconductors (europium chalcogenides) with unique electronic, magnetic, optical, and magneto-optical (MO) properties.[14] For applications in optoelectronics, it is particularly significant that the band gap of EuO at room temperature is 1.12 eV, which is comparable to that of silicon, which would allow spin-polarized electronic injection.[15] These special features have opened prospects for the fabrication of optoelectronic and spintronic devices based on EuO, which would be compatible with the current CMOS semiconductor technology.[16] However, most of these attractive properties have been studied in high-quality monocrystalline EuO thin films,[17] which is difficult and costly to prepare.[18] In this context, there has been insufficient research related to the study of the magnetic and optical properties of nanocrystalline and nanodimensional EuO and might have new and unexpected properties. Additionally, the preparation of nanocrystalline EuO films following a relatively simple procedure would be highly desirable. Note that, by preparing light emitting pure Eu-based films, the effective number of emitting ions per unit volume can be effectively increased compared to that in Eu-doped materials. In this regard, we have recently shown the successful preparation of

Received: April 6, 2020
Revised: June 2, 2020
Published: June 16, 2020

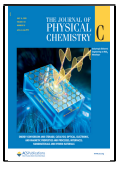

transparent nanocrystalline EuO thin films in the near infrared, which expands the potential for optical applications of this material.[19] However, the potential of light emission of nano-EuO_x films has not been yet addressed, although ions are generally used as dopant for phosphors in lighting application because of their extraordinary emission properties. In previous works, the tuning of the luminescence europium-doped oxides, for example, silicon oxides[20] and $CaYAlO_4$,[21] has been investigated as a function of the annealing conditions. In particular, the emission of Eu^{3+} ions consists of narrow emission peaks with long lifetimes originated from the intra-4f electronic transitions. By contrast, the emission of the Eu^{2+} ions shows a broad band with short lifetimes influenced by a strong dependence of the host matrix[2] because the 5d orbitals of Eu^{2+} ions are very sensitive to the changes of the surroundings due to them being in the outer electronic shell compared with the inner 4f orbitals. For the specific case of the crystalline EuO (an ionic crystal with a rock-salt structure with Eu cations octahedrally coordinated by oxygen anions), Eu cations exhibit a 2+ oxidization state. The ligand crystal field splits the empty 5d shells into a lower t_{2g} triplet and an upper e_g, forming the conduction band of EuO.[22] In this work, we perform a comprehensive study of the photoluminescence light emission of EuO_x thin films formed by nanocrystals and prepared at room temperature with no post-annealing treatment. These nano-EuO_x thin films are fabricated following a flexible and straightforward deposition procedure that allows a fine-tuning of their oxygen content by adjusting the background pressure in the vacuum chamber during pulsed laser deposition. In addition, we encapsulate the films with a protective layer of Al_2O_3 to prevent the EuO_x thin film transformation once they are in contact with the ambient pressure, preserving their original stoichiometry and quality. Interestingly, the optical emission energy (color) of nano-EuO_x films can be tailored in the visible spectrum by controlling their stoichiometry. These experimental findings open new perspectives for the fabrication of nano-EuO_x films for their integration with silicon as wide tunable "one-compound" ultrathin emitters.

METHODS

EuO_x films with a nominal thickness of 100 nm have been prepared by pulsed laser deposition (PLD) using an ultraviolet Argon-Fluor excimer laser (λ = 193 nm; 20 ns pulse duration) focused on a Eu_2O_3 target with an energy density of 1.4 ± 0.2 J/cm^2 at a repetition rate of 10 Hz on Si (100) substrates held at room temperature.[23] The base pressure in the vacuum chamber has been changed in the 10^{-7} to 10^{-6} mbar range. To isolate the EuO_x nanocrystals from ambient conditions and hinder their oxidation upon exposure to air, the EuO_x deposits have been capped with a 15 nm-thick amorphous Al_2O_3 protecting film. We have found that this encapsulation procedure is crucial to preserve the stoichiometry of the EuO_x films, as detailed below. The stoichiometry of the EuO_x nanocrystals has been assessed by X-ray photoemission spectroscopy (XPS) measurements using a Theta Probe XPS system from Thermo Fisher Scientific with monochromatic 1486.6 eV Al-Kα X-rays operated at 15 kV and an emission current of 6.7 mA. For the measurements, we have used a maximum spot size of the X-ray beam of 400 μm in diameter and a constant energy mode with a constant pass energy of 50 eV (1.00 eV full width at a half-maximum on Ag $3d_{5/2}$). The X-ray diffraction study of the EuO_x nanocrystals has been performed with Philips X'Pert MPD equipment in the θ–2θ configuration (1.5406 Å, Cu Kα). Structural analysis of the EuO_x has been also performed by means of high-resolution transmission electron microscopy (HRTEM) techniques, including Z-contrast scanning TEM (STEM) mode using a high-angle annular detector (HAADF) and high-resolution energy dispersive X-ray spectroscopy (EDS). The following procedure has been applied for the preparation of the TEM specimens: (i) deposition of a (15–20) nm of EuO_x on a microscopy grid—the Si (100) grid is hexagonal 200 μm thick and has a 50 nm-thick amorphous SiN membrane at its center; (ii) deposition of a 15 nm-thick Al_2O_3 protective layer on the EuO_x film. In this way, the EuO_x film is protected by the SiN membrane at the bottom and by the Al_2O_3 layer on the top. To avoid electron beam-induced damage or modifications of the EuO_x film crystal structure, the electron beam is kept at low electron density and short exposition times. The crystal structure and phase identification have been obtained from fast Fourier transform (FFTs) analysis of high-resolution TEM images. The photoluminescence (PL) measurements have been carried out under excitation at λ = 355 nm at a nominal power of 100 mW (spot of 1 mm) from a solid-state Genesis CX 355-200 optically pumped semiconductor laser (Coherent). The light emitted by the EuO_x nanocrystals has been collected by a microscope objective (10× Mitutoyo Plan Apo NIR infinity-corrected objective), focalized over a Czerny–Turner-type monochromator (Acton Spectra Pro 300i, with a diffraction grating of 1200 g/mm) and detected through a photomultiplier EMI 9659QB. The signal is amplified with the conventional lock-in technique and collected by a LabVIEW program. In addition, the chromatic coordinates of the emission have been analyzed. For this purpose, the three-color matching functions established by the Commission Internationale de l'Éclairage (CIE) in 1931, i.e., CIE 1931 x-y color matching functions, have been used.[24] The chromatic coordinates are calculated by means of a MATLAB script.[25]

RESULTS AND DISCUSSION

Figure 1a shows the XPS spectra corresponding to the Eu 3d nuclear level for a set of films prepared under the base

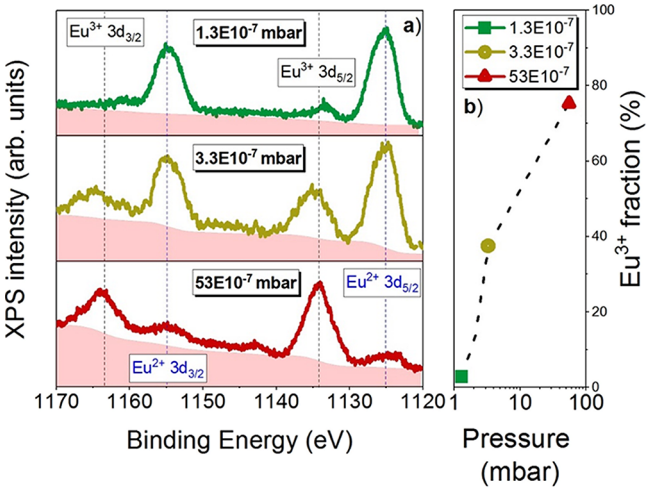

Figure 1. (a) XPS 3d spectra: Eu^{2+} and Eu^{3+} contributions are marked by dashed lines. The pink shadow area represents the signal background. (b) Eu^{3+} relative percentage fraction in the logarithmic scale for films grown at 1.3, 3.3, and 53 (·10^{-7} mbar).

https://dx.doi.org/10.1021/acs.jpcc.0c03052
J. Phys. Chem. C 2020, 124, 15434–15439

pressures of 1.3×10^{-7}, 3.3×10^{-7}, and 53×10^{-7} mbar. Four peaks are observed in the spectra, Eu^{2+} $3d_{5/2}$ and $3d_{3/2}$ and Eu^{3+} $3d_{5/2}$ and $3d_{3/2}$. The emissions centered around 1125 and 1155 eV are assigned to the components due to the spin−orbit coupling of EuO_x in the 2+ state, i.e., Eu^{2+} $3d_{5/2}$ and $3d_{3/2}$, with a spin−orbit splitting of (30 ± 1) eV. The asymmetry of the peaks is attributed to (i) the presence of the divalent multiplet of the $3d^9$ $4f^7$ final state and (ii) photoelectron energy loss at higher binding energies with respect to the multiplet from a shake-up process, as reported for divalent Eu compounds,[26] and specifically in EuO thin films grown by MBE (molecular beam epitaxy).[27] The other two remaining peaks, centered around 1134 and 1163 eV, correspond to the trivalent doublet, Eu^{3+} $3d_{5/2}$ and $3d_{3/2}$, i.e., to the components due to the spin−orbit coupling of EuO_x in the 3+ state.

In the analysis of the XPS data in Figure 1, we assume a similar contribution of the cross section for the 3d core level of Eu^{3+} and Eu^{2+} peaks (Caspers et al.,[27] Zavala-Sanchez et al.,[28] and Kumar et al.[29]). Hence, the fraction of Eu in the 3+ state has been determined considering the integrated spectral intensities (areas under the curve) of the peaks, yielding

$$f^{Eu^{3+}} = \left(\frac{\sum A^{Eu^{3+}}}{\sum A^{Eu^{2+}} + \sum A^{Eu^{3+}}} \right) \times 100 \quad (1)$$

where $\sum A^{Eu^{3+}}$ is the sum of the areas under the Eu^{3+} curves peaked at 1134 and 1163 eV and $\sum A^{Eu^{2+}}$ is the sum of the areas under the Eu^{2+} curves peaked at 1125 and 1155 eV. In Figure 1b, the values calculated using eq 1 with an uncertainty of ≈5% are represented as a function of the background pressure during growth. With increasing the background pressure in the chamber, the oxygen content in the films also rises, as confirmed by the enhancement of intensity of the peaks corresponding to the Eu^{3+} oxidation state, with respect to those related to the 2+ oxidation state. The 1.3 EuO_x film (grown at a pressure of $1.3 \cdot 10^{-7}$) mbar presents a Eu^{3+} relative percentage fraction of 2.7%, i.e., it consists of 97.3% EuO and 2.7% Eu^{3+}, and therefore, we can conclude that it is essentially stoichiometric EuO. The relatively low amount of Eu^{3+} in the film is even lower than the 4% recently reported for nominally stoichiometric EuO.[27] In contrast, when analyzing the film deposited at the highest pressure ($53 \cdot 10^{-7}$ mbar), it is found that the contribution from Eu^{2+} is considerably reduced in comparison to 1.3 film and the spectrum is dominated by the emissions from Eu^{3+}. Here, the Eu^{3+} relative percentage fraction is 75.3%, giving 24.7% of EuO in the film. The 3.3 film (grown at $3.3 \cdot 10^{-7}$ mbar) contains an Eu^{3+} relative percentage fraction of 37.5%. These results confirm that the stoichiometry of the films can be suitably controlled by adjusting the base pressure in the growth chamber, showing consistent results with our previous work.[30] Therefore, according to the XPS data, the stoichiometry of the films is EuO for the 1.3 film, $EuO_{1.2}$ for the 3.3 film, and $EuO_{1.4}$ (close to Eu_2O_3) for the 53 film. The process that enables the preparation of EuO_x with a different oxygen content by controlling the base pressure during deposition is linked to the special characteristics of the plasma created by the laser ablation. The basic concept is that, starting from a target with a Eu_2O_3 stoichiometry and performing the deposition in vacuum, there is an oxygen loss process when the laser plasma is formed, and as a consequence, reduced EuO films can be produced if the base vacuum is low enough. By increasing the base pressure, it is possible to obtain films of fully oxidized Eu_2O_3. However, it is also necessary to understand the underlying physics that leads to the formation of the EuO_x thin films at room temperature. The Gibbs free energy (GfE) of formation in standard material states is given by the equations

$$\Delta G_f^\circ = \Delta H_f^\circ - T\Delta S^\circ \quad (2)$$

$$\Delta H_f^\circ = \sum_i^a n_i \Delta H_{f-\text{products}}^\circ - \sum_j^b m_j \Delta H_{f-\text{reagents}}^\circ \quad (3)$$

$$\Delta S^\circ = \sum_i^a n_i S_{\text{products}}^\circ - \sum_j^b m_j S_{\text{reagents}}^\circ \quad (4)$$

where ΔG_f° represents the GfE of formation, ΔH_f° and ΔS° are the enthalpy and entropy variations, respectively, and T is the temperature. In this work, we are changing the base pressure, and therefore, we can determine the change in the Gibbs free energy due to a change in pressures at constant temperature through

$$\Delta G_f = G(p_f) - G(p_i) = \int_{p_i}^{p_f} V dP \quad (5)$$

where p_f and p_i are the final and initial pressures, respectively, and V is the material volume. For our case, we can use the GfE of formation in standard states (298 K and 1 atm) to discuss the results because the sensitivity of GfE to changes in pressure is negligible for solids (this means that V may be treated as a constant and taken outside the integral in eq 5). The GfE of formation in standard states of Eu_2O_3 and EuO are −1565 and −557 kJ·mol^{-1}, respectively.[31] The negative values are in agreement with the observed spontaneous formation of our compounds. From these values, it follows that the Eu_2O_3 is the most stable phase, and therefore, it should be the dominant phase in the films. However, under a base pressure of $1.3 \cdot 10^{-7}$ mbar, the lowest used in this work, the films have EuO composition. Therefore, in the plasma generated by the laser ablation upon vaporization of the Eu_2O_3 target, the oxygen are more easily deflected that the europium species in the plasma collisions and fails to reach the substrate.[32] In these conditions, EuO films are formed. When the base pressure is increased, the plasma generated by the laser is more confined due to the residual vapor pressure in the chamber, and less oxygen is deviated in the collision processes and more oxygen species reach the substrate. In these conditions, rich EuO_x films ($1 < x < 3/2$) are formed. As long as the films remain in the vacuum chamber, the formed films are stable; however, because GfE (Eu_2O_3) < GfE (EuO) in ambient conditions, i.e., oxygen-rich atmosphere, the oxidation of the EuO is dramatically enhanced. Ideally, to keep the desired stoichiometry unaltered in the as-grown film when exposed to air, a protective encapsulating coating would be highly desirable. In our films, this is provided by a Al_2O_3 nanometer-thick layer owing to its higher value of GfE (−1582 kJ·mol^{-1}) in comparison with that of EuO, which makes unlikely its reaction with the underlying EuO_x thin films.

To gain a deeper insight into the structure of the films, XRD measurements have been performed on the EuO_x films, confirming the presence EuO nanocrystals with average sizes of ≈5−7 (± 1) nm, obtained by means of the Scherrer equation, independently of the background pressure used during deposition. Details on the XRD measurements are

https://dx.doi.org/10.1021/acs.jpcc.0c03052
J. Phys. Chem. C 2020, 124, 15434−15439

provided in the Supporting Information. In particular, the XRD spectra show broad peaks corresponding to EuO nanocrystals with crystalline planes (111) and (220) for the EuO and $EuO_{1.2}$ thin films and only EuO nanocrystals with the crystalline plane (111) for the $EuO_{1.4}$ thin film. In the following, we will refer to the films by their composition. In Figure 2a, a representative image of the HRTEM measurements is reported. The detailed HRTEM analysis has been performed on the $EuO_{1.2}$ because it is the most interesting film and, according to the XPS and XRD analyses, contains Eu both in the 2+ and 3+ oxidation states. The FFT of this figure is given in Figure 2b where the reflections corresponding to nanocrystals with a NaCl structure are resolved, orientated along the [011] zone axis for the (220) crystalline plane and [001] for the (200) crystalline plane, and a lattice parameter of $a_0 = 5.14 \pm 0.02$ Å, comparable to the one of bulk EuO. The intermediate areas are represented in a blue color, and the brighter FFT spots correspond to the (222) planes in Eu_2O_3 with a lattice spacing of (3.15 ± 0.02) Å and a lattice parameter $a_0 = (10.86 \pm 0.02)$ Å. As evidenced in Figure 2b, the Eu_2O_3 regions, together with the noncrystallized zones (dark zones), are situated in the free volume between the EuO nanocrystals. The Al_2O_3 protecting layer (not shown) is found to be amorphous, as already reported for PLD deposited films.[33] In Figure 2c, it is shown through a high-resolution detail of the EuO nanocrystal where the interatomic planes are resolved with an interplanar distance of 2.58 Å (theoretical value of 2.57 Å). These results indicate the formation of EuO nanocrystals surrounded by Eu_2O_3 nanocrystalline and amorphous regions. The HRTEM observations are in excellent agreement with the XRD analysis that showed the formation of nanocrystals with average sizes in the 5−7 (±1) nm range. The TEM analysis is in good agreement with the XPS results that show the coexistence of Eu^{2+} and Eu^{3+} oxidation states.

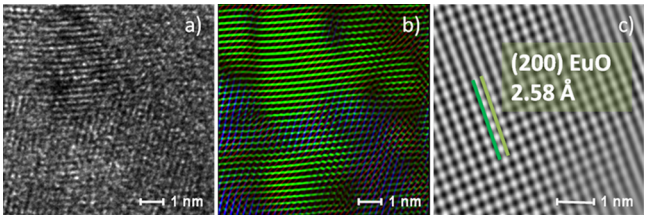

Figure 2. (a) HRTEM image of the film ($EuO_{1.2}$). (b) FFT-filtered TEM image. In green color: EuO nanocrystals with the (220) and (200) crystalline orientations. In blue color: nanocrystalline Eu_2O_3 areas. (c) Detail of a EuO nanocrystal (green zone in panel b) with the (200) crystalline orientation.

Photoluminescence (PL) measurements have been performed under an ultraviolet laser (λ = 355 nm) to obtain the optical emission of the EuO_x thin films. It is known that the luminescent properties of the europium ions depend on their valence state. In particular, the emission of Eu^{3+} ions shows a series of narrow emission peaks with long lifetimes, i.e., electronic transitions $^5D_0 \rightarrow {}^7F_J$ (J = 0, 1, 2, 3, 4, 5, 6) of the 4f orbitals.[4] However, the emission of the Eu^{2+} ions is characterized by a broad emission band with short lifetimes due to the transitions of the electrons from the 5d to the 4f orbitals. Figure 3a shows the visible (VIS) photoluminescence of the EuO_x thin films displaying a different behavior depending on the oxidation state for EuO, $EuO_{1.2}$, and $EuO_{1.4}$ thin films. In particular, EuO shows a broadband emission centered in ≈525 nm associated to the 5d → 4f electronic transitions.[34] The $EuO_{1.2}$ thin film in which both 2+ and 3+ oxidation states are found to be relevant according to the XPS and HRTEM analysis presents a mixture behavior. First, there are two bands centered at ≈460 and 560 nm, which are associated to emissions of the 5d → 4f electronic transitions of the Eu^{2+} ions. Second, there is a small and narrow emission line at 615 nm, attributed to the emission of intra-4f transitions of the Eu^{3+} ions. At this point, it is important to note that the 5d orbitals of Eu^{2+} ions are very sensitive to the changes of the crystal field because they are in the outer electronic shell compared with the inner 4f orbitals. It is reported also that the incorporation of oxygen on the nanocrystals surface has strong consequences as it modifies the concentration of charge carriers, thus affecting the electronic,[35] magnetic,[36] and optical properties.[37] Therefore, the emission spectra strongly depend on the nature of the Eu^{2+} surroundings.[38] Indeed, by means of HRTEM, we found EuO nanocrystals surrounded by both amorphous and crystalline areas, which affects differently to the configuration of the 5d orbitals, which would explain the two emission bands found in the $EuO_{1.2}$ PL spectrum. Finally, the spectrum of the $EuO_{1.4}$ thin film presents narrow emissions corresponding to Eu in the 3+ oxidation state associated to $^5D_0 \rightarrow {}^7F_2$ intra-4f electronic transitions,[39] which is also in agreement with the XPS results. The emission trend of the films as a function of

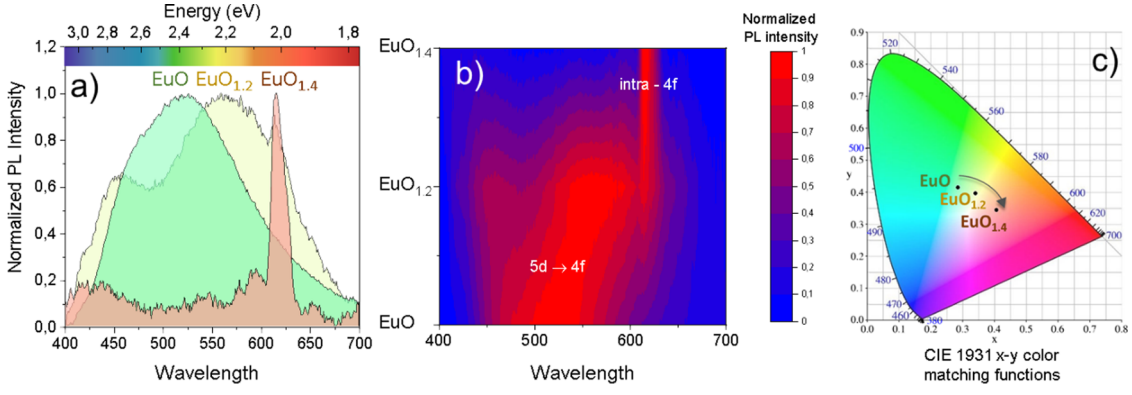

Figure 3. (a) Photoluminescence spectra and (b) interpolated PL intensity map of the EuO_x films obtained under UV (355 nm) laser excitation. (c) The filled color of each graph represents the color emission established by the Commission Internationale de l'Éclairage (CIE) in 1931, known as the CIE 1931. (b) CIE 1931 x-y color matching functions for the corresponding EuO_x thin films.

https://dx.doi.org/10.1021/acs.jpcc.0c03052
J. Phys. Chem. C 2020, 124, 15434−15439

their oxygen content is more clearly seen in Figure 3b where an interpolated intensity map of the emission is represented. The main PL contribution for the EuO film (centered in ≈525 nm) is shifted to the red to ≈550 nm for the $EuO_{1.2}$ thin film, i.e., as the oxidation state in the surroundings of the EuO nanocrystals increases. This is further verified by the emission of the Eu ions in the 3+ oxidation state, as observed in the PL spectrum by the narrow emission in 615 nm. Finally, for the most oxidized sample, the $EuO_{1.4}$ thin film, we only find emission of Eu ions in the 3+ oxidation state. Hence, these results are in perfect agreement with XPS, XRD, and HRTEM analysis where we can control the oxidation state by setting the base pressure, eventually leading to a tuning of the optical emission.

To determine the visible "color" emission of the EuO_x thin films, we have calculated the chromatic coordinates of the photoluminescence using a MATLAB script.[25] For this purpose, we have chosen the three-color matching functions established by the Commission Internationale de l'Éclairage (CIE) in 1931, i.e., the CIE 1931 *x-y* color matching functions.[24] The resulting chromaticity plot is represented in Figure 3c and shows the eye perception of color emission for each thin film. It is remarkable for the broad emission spectrum obtained for the films EuO (green) and $EuO_{1.2}$ (yellow), which is intrinsically related to the surroundings of the Eu^{2+} ions present in the films.[38] In contrast, the color of the nanostructured $EuO_{1.4}$ thin film presents a narrow and pure red emission attributed to the intra-4f transitions of the Eu^{3+} ions. The results confirm the possibility of shifting the color emission from green to red by controlling the Eu oxidation state, opening a way to the fine-tuning of the visible emission for the development of optically active nanometer-sized emitters integrated on silicon, which are very promising for one-compound nanostructured displays.

CONCLUSIONS

In this work, we have prepared EuO_x films that show tunable photoluminescence by varying their stoichiometry in a wide range ($1 \leq x < 1.4$). The compositional and structural analysis show that they are formed by EuO_x nanocrystals. The different nominal stoichiometries have been successfully achieved by simply controlling the background pressures of the vacuum chamber from $1.3 \cdot 10^{-7}$ mbar (EuO) to pressures above $53 \cdot 10^{-7}$ mbar ($EuO_{1.4}$). The photoluminescence light emission of the EuO_x films evolves from a broadband band centered in the green attributed to 5d → 4f transitions of Eu^{2+} ions to a narrow red emission attributed to the intra-4f transitions of the Eu^{3+} ions. The experimental findings reported in this work open wide perspectives of nanodimensional EuO_x films for "one-component" tunable optoelectronic applications for their incorporation in integrated silicon-based devices.

ASSOCIATED CONTENT

Supporting Information

The Supporting Information is available free of charge at https://pubs.acs.org/doi/10.1021/acs.jpcc.0c03052.

Information about the analysis and discussion of the XRD data (PDF)

AUTHOR INFORMATION

Corresponding Authors

Antonio Mariscal-Jiménez − *Laser Processing Group, Instituto de Óptica, IO-CSIC, 28006 Madrid, Spain; Departamento de Tecnologías de la Información, Escuela Politécnica Superior, Universidad CEU-San Pablo, CEU Universities, Campus Montepríncipe, Boadilla del Monte, Madrid 28668, Spain;* orcid.org/0000-0002-7178-1452; Email: antonio.mariscal@csic.es

Javier Martín-Sánchez − *Institut für Halbleiter-und-Festkörperphysik, Johannes Kepler University, A-4040 Linz, Austria; Departamento de Física, Universidad de Oviedo, 33007 Oviedo, Spain; Center of Research on Nanomaterials and Nanotechnology, CINN (CSIC−Universidad de Oviedo), El Entrego 33940, Spain*; Email: javiermartin@uniovi.es

Rosalía Serna − *Laser Processing Group, Instituto de Óptica, IO-CSIC, 28006 Madrid, Spain;* orcid.org/0000-0002-7101-3947; Email: rosalia.serna@csic.es

Authors

Aitana Tarazaga Martín-Luengo − *Institut für Halbleiter-und-Festkörperphysik, Johannes Kepler University, A-4040 Linz, Austria*

Beatriz Galiana − *Department of Physics, Escuela Politécnica Superior, Universidad Carlos III, 28911 Leganés, Madrid, Spain*

Carmen Ballesteros − *Department of Physics, Escuela Politécnica Superior, Universidad Carlos III, 28911 Leganés, Madrid, Spain*

Alberta Bonanni − *Institut für Halbleiter-und-Festkörperphysik, Johannes Kepler University, A-4040 Linz, Austria*

Complete contact information is available at: https://pubs.acs.org/10.1021/acs.jpcc.0c03052

Notes

The authors declare no competing financial interest.

ACKNOWLEDGMENTS

This work has been financially supported by the Spanish Ministerio de Ciencia e Innovación through grant RTI2018-096498-B-I00 (MCIU/AEI/FEDER, UE). Support by the EC's Horizon 2020 Research and Innovation Programme (grant 645776), by the Austrian Science Fund (FWF) (P24471 and P26830), and by the NATO Science for Peace Programme (grant 984735) is acknowledged. A.M-J. acknowledges the financial support through BES-2013-062593. J.M-S acknowledges financial support through the Ramón y Cajal Program from the Government of Spain and FSE (RYC2018-026196-I). We acknowledge support of the publication fee by the Austrian Science Fund (FWF) Der Wissenschaftsfonds Open Access Publication Support Initiative.

REFERENCES

(1) Feng, P. F.; Kong, M. Y.; Yang, Y. W.; Su, P. R.; Shan, C. F.; Yang, X. X.; Cao, J.; Liu, W. S.; Feng, W.; Tang, Y. Eu 2+ /Eu 3+ -Based Smart Duplicate Responsive Stimuli and Time-Gated Nanohybrid for Optical Recording and Encryption. *ACS Appl. Mater. Interfaces* **2019**, *11*, 1247−1253.

(2) Camps, I.; Mariscal, A.; Calvo-Barrio, L.; Serna, R. White Cathodoluminescence Emission from Eu-Doped SiAlON Thin Films. *Phys. Status Solidi Appl. Mater. Sci.* **2018**, *215*, 1800260.

(3) Dutta, S.; Som, S.; Meena, M. L.; Chaurasiya, R.; Chen, T. M. Multisite-Occupancy-Driven Intense Narrow-Band Blue Emission from Sr5SiO4Cl6:Eu2+ Phosphor with Excellent Stability and Color Performance. *Inorg. Chem.* **2020**, 1928.

(4) Kenyon, A. J. Recent Developments in Rare-Earth Doped Materials for Optoelectronics. *Prog. Quantum Electron.* **2002**, *26*, 225−284.

(5) López, I.; Lorenz, K.; Nogales, E.; Méndez, B.; Piqueras, J.; Alves, E.; García, J. A. Study of the Relationship between Crystal Structure and Luminescence in Rare-Earth-Implanted Ga2O3 Nanowires during Annealing Treatments. *J. Mater. Sci.* **2014**, *49*, 1279−1285.
(6) Zhao, Y.; Xie, R. J.; Dierre, B.; Takeda, T.; Sekiguchi, T.; Hirosaki, N.; Wang, L. Enhanced Cathodoluminescence of Green β-Sialon:Eu2+phosphor by In2O3coating. *J. Alloys Compd.* **2017**, *727*, 1110−1114.
(7) Van De Haar, M. A.; Berends, A. C.; Krames, M. R.; Chepyga, L.; Rabouw, F. T.; Meijerink, A. Eu3+ Sensitization via Nonradiative Interparticle Energy Transfer Using Inorganic Nanoparticles. *J. Phys. Chem. Lett.* **2020**, 689−695.
(8) Zhu, Q. Q.; Yang, P. F.; Wang, Z. Y.; Hu, P. C. Additive-Free Y2O3:Eu3+ Red-Emitting Transparent Ceramic with Superior Thermal Conductivity for High-Power UV LEDs and UV LDs. *J. Eur. Ceram. Soc.* **2020**, 2426.
(9) Janulevicius, M.; Marmokas, P.; Misevicius, M.; Grigorjevaite, J.; Mikoliunaite, L.; Sakirzanovas, S.; Katelnikovas, A. Luminescence and Luminescence Quenching of Highly Efficient Y2Mo4O15:Eu3+ Phosphors and Ceramics. *Sci. Rep.* **2016**, *6*, 26098.
(10) Quesada, A.; del Campo, A.; Fernández, J. F. Sintering Behaviour and Translucency of Dense Eu2O3 Ceramics. *J. Eur. Ceram. Soc.* **2014**, *34*, 1803−1808.
(11) Zhou, X.; Zhang, K. H.; Xiong, J.; Park, J. H.; Dickerson, J. H.; He, W. Size- and Dimensionality-Dependent Optical, Magnetic and Magneto-Optical Properties of Binary Europium-Based Nanocrystals: EuX (X = O, S, Se, Te). *Nanotechnology* **2016**, *27*, 192001.
(12) Formisano, F.; Medapalli, R.; Xiao, Y.; Ren, H.; Fullerton, E. E.; Kimel, A. V. Femtosecond Magneto-Optics of EuO. *J. Magn. Magn. Mater.* **2020**, *502*, 166479.
(13) Averyanov, D. V.; Sokolov, I. S.; Tokmachev, A. M.; Parfenov, O. E.; Karateev, I. A.; Taldenkov, A. N.; Storchak, V. G. High-Temperature Magnetism in Graphene Induced by Proximity to EuO. *ACS Appl. Mater. Interfaces* **2018**, *10*, 20767−20774.
(14) Pavlov, V. V. Linear and Nonlinear Magneto-Optical Phenomena in Epitaxial Films of Europium Chalcogenides EuX (X = O, Se, Te). *Phys. Solid State* **2019**, *61*, 408−413.
(15) Lev, L. L.; Averyanov, D. V.; Tokmachev, A. M.; Bisti, F.; Rogalev, V. A.; Strocov, V. N.; Storchak, V. G. Band Structure of the EuO/Si Interface: Justification for Silicon Spintronics. *J. Mater. Chem. C* **2017**, *5*, 192−200.
(16) Averyanov, D. V.; Sadofyev, Y. G.; Tokmachev, A. M.; Primenko, A. E.; Likhachev, I. A.; Storchak, V. G. Direct Epitaxial Integration of the Ferromagnetic Semiconductor EuO with Silicon for Spintronic Applications. *ACS Appl. Mater. Interfaces* **2015**, *7*, 6146−6152.
(17) Averyanov, D. V.; Karateeva, C. G.; Karateev, I. A.; Tokmachev, A. M.; Kuzmin, M. V.; Laukkanen, P.; Vasiliev, A. L.; Storchak, V. G. A Prospective Submonolayer Template Structure for Integration of Functional Oxides with Silicon. *Mater. Des.* **2017**, *116*, 616−621.
(18) Caspers, C.; Gloskovskii, A.; Gorgoi, M.; Besson, C.; Luysberg, M.; Rushchanskii, K. Z.; Ležaić, M.; Fadley, C. S.; Drube, W.; Müller, M. Interface Engineering to Create a Strong Spin Filter Contact to Silicon. *Sci. Rep.* **2016**, *6*, 22912.
(19) Mariscal, A.; Quesada, A.; Martín-Luengo, A. T.; García, M. A.; Bonanni, A.; Fernández, J. F.; Serna, R. Europium Monoxide Nanocrystalline Thin Films with High Near-Infrared Transparency. *Appl. Surf. Sci.* **2018**, *456*, 980−984.
(20) Li, D.; Zhang, X.; Jin, L.; Yang, D. Structure and Luminescence Evolution of Annealed Europium-Doped Silicon Oxides Films. *Opt. Express* **2010**, *18*, 27191.
(21) Zhang, Y.; Li, X.; Li, K.; Lian, H.; Shang, M.; Lin, J. Crystal-Site Engineering Control for the Reduction of Eu3+ to Eu2+ in CaYAlO4: Structure Refinement and Tunable Emission Properties. *ACS Appl. Mater. Interfaces* **2015**, *7*, 2715−2725.
(22) Güntherodt, G. Optical Properties and Electronic Structure of Europium Chalcogenides. *Phys. Condens. Matter* **1974**, *18*, 37−78.
(23) De Sande, J. C. G.; Serna, R.; Gonzalo, J.; Afonso, C. N.; Hole, D. E.; Naudon, A. Refractive Index of Ag Nanocrystals Composite Films in the Neighborhood of the Surface Plasmon Resonance. *J. Appl. Phys.* **2002**, *91*, 1536−1541.
(24) Luo, R. *Encyclopedia of Color Science and Technology*; Springer Publishing Company, 2016. DOI: 10.1007/978-3-642-27851-8.
(25) Patil, P.. *CIE Coordinate Calculator - File Exchange - MATLAB Central* https://es.mathworks.com/matlabcentral/fileexchange/29620-cie-coordinate-calculator (accessed 2018-12-21).
(26) Cho, E. J.; Oh, S. J.; Imada, S.; Suga, S.; Suzuki, T.; Kasuya, T. Origin of the High-Binding-Energy Structure in the 3d Core-Level Spectra of Divalent Eu Compounds. *Phys. Rev. B* **1995**, *51*, 10146−10149.
(27) Caspers, C.; Müller, M.; Gray, A. X.; Kaiser, A. M.; Gloskovskii, A.; Fadley, C. S.; Drube, W.; Schneider, C. M. Chemical Stability of the Magnetic Oxide EuO Directly on Silicon Observed by Hard X-Ray Photoemission Spectroscopy. *Phys. Rev. B* **2011**, *84*, 205217.
(28) Zavala-Sanchez, L. A.; Hirata, G. A.; Novitskaya, E.; Karandikar, K.; Herrera, M.; Graeve, O. A. Distribution of Eu2+ and Eu3+ Ions in Hydroxyapatite: A Cathodoluminescence and Raman Study. *ACS Biomater. Sci. Eng.* **2015**, *1*, 1306−1313.
(29) Kumar, S.; Prakash, R.; Choudhary, R. J.; Phase, D. M. Structural, XPS and Magnetic Studies of Pulsed Laser Deposited Fe Doped Eu2O3 Thin Film. *Mater. Res. Bull.* **2015**, *70*, 392−396.
(30) Mariscal, A.; Quesada, A.; Camps, I.; Palomares, F. J.; Fernández, J. F.; Serna, R. Tuning Eu3+emission in Europium Sesquioxide Films by Changing the Crystalline Phase. *Appl. Surf. Sci.* **2016**, *374*, 71−76.
(31) Lide, D. R. *CRC Handbook of Chemistry and Physics, 84th Edition; CRC HANDBOOK OF CHEMISTRY AND PHYSICS*; Taylor & Francis, 2003.
(32) Gomez-San Roman, R.; Casero, R. P.; Maréchal, C.; Enard, J. P.; Perrière, J. 18O Isotopic Tracer Studies of the Laser Ablation of Bi2Sr2Ca1Cu2O8. *J. Appl. Phys.* **1996**, *80*, 1787−1793.
(33) Núñez-Sánchez, S.; Serna, R.; López, J. G.; Petford-Long, A. K.; Tanase, M.; Kabius, B. Tuning the Er3+ Sensitization by Si Nanoparticles in Nanostructured As-Grown Al2 O3 Films. *J. Appl. Phys.* **2009**, *105*, 013118.
(34) Camps, I.; Mariscal, A.; Serna, R. Preparation and Broadband White Emission of Eu-Doped Thin Films Based on SiAlON. *J. Lumin.* **2017**, *191*, 97−101.
(35) Lee, W.; Jung, H. J.; Lee, M. H.; Kim, Y.-B.; Park, J. S.; Sinclair, R.; Prinz, F. B. Oxygen Surface Exchange at Grain Boundaries of Oxide Ion Conductors. *Adv. Funct. Mater.* **2012**, *22*, 965−971.
(36) Wannasen, L.; Swatsitang, E. Magnetic Properties Dependence on Fe2+/Fe3+ and Oxygen Vacancies in SrTi0.95Fe0.05O3 Nanocrystalline Prepared by Hydrothermal Method. *Microelectron. Eng.* **2015**, *146*, 92−98.
(37) Bryant, G. W.; Jaskolski, W. Surface Effects on Capped and Uncapped Nanocrystals. *J. Phys. Chem. B* **2005**, *109*, 19650−19656.
(38) Poort, S. H. M.; Blasse, G. The Influence of the Host Lattice on the Luminescence of Divalent Europium. *J. Lumin.* **1997**, *72-74*, 247−249.
(39) Geng, D.; Lozano, G.; Míguez, H. Highly Efficient Transparent Nanophosphor Films for Tunable White-Light-Emitting Layered Coatings. *ACS Appl. Mater. Interfaces* **2019**, *11*, 4219−4225.